33rd Annual International Conference of the IEEE EMBS
Boston, Massachusetts USA, August 30 - September 3, 2011

ECG-based detection of body position changes using a Laplacian noise model

Ana Mincholé, Leif Sörnmo and Pablo Laguna

***Abstract*— Body position changes (BPC), which are often manifested in the ECG as shifts in the electrical axis of the heart, result in ST changes, and thus, may be misclassified as ischemic events during ambulatory monitoring. We have developed a BPC detector by modeling shifts as changes in the Karhunen-Loève transform coefficients of the QRS complex and the ST-T waveform. The noise is assumed to have a Laplacian distribution. A generalized likelihood ratio test has been chosen as the strategy to detect BPCs. Two different databases have been used to assess detection performance. The obtained results were 93%/99% in terms of sensitivity/positive predictivity value (S/+PV) and a false alarm rate of 2 events/hour. The results clearly outperform current techniques (S/+PV: 85%/99%) based on the Gaussian noise assumption.**

I. INTRODUCTION

Electrocardiographic variations due to body position changes (BPCs) are problematic in ambulatory recordings and during ST monitoring. Rotation of the heart relative to the electrode location of the electrocardiogram (ECG) when a patient turns from one side to another has been reported to cause ST-segment shifts, triggering false ischemic alarms with continuous ST-segment monitoring [1]. In this work, we have implemented a BPC detector for use in ST monitoring to cancel false positives in ischemia detection.

BPCs produce significant changes in the ECG signal, especially in the QRS complex and the ST-T waveform [2]. In order to track such morphological changes, BPC detectors may be based on the Karhunen-Loève transform (KLT), in which most of the signal information, in terms of energy, is concentrated to a few coefficients. BPCs are manifested as step-like changes in the KLT coefficient series of the QRS and ST-T complexes [3].

In this study, the KLT of the QRS complex and the ST-T waveform are used to develop a BPC detector based on the generalized likelihood ratio test (GLRT).

II. METHODS

A. GLRT based detector

The GLRT-based detection strategy consists of the following stages:

This work was supported by Ministerio de Ciencia y Tecnología, FEDER under Project CICYT TEC2010-21703-C03-02

A. Mincholé and P. Laguna are with CIBER-BBN, GTC, I3A, IIS Aragón and Universidad de Zaragoza, Zaragoza, Spain minchole@unizar.es

L. Sörnmo is with Dept. of Electrical and Information Technology, Lund University, Sweden.

1) Preprocessing Stage:

- ECG baseline wander attenuation using cubic splines.
- Synthesis of vectorcardiographic (VCG) leads obtained from the 12-lead ECG, using the inverse Dower matrix.
- QRS fiducial point detection [4].
- Rejection of beats with low signal-to-noise ratio (SNR), estimated as the ratio between peak-to-peak QRS amplitude and the RMS value of the high-frequency noise (above 25 Hz), differing more than 20 dB from the exponentially averaged SNR. The forgetting factor of the exponential averaging is set to 0.02.
- Rejection of beats with differences in mean isoelectric level with respect to adjacent beats exceeding 400 μV.
- QRS and ST-T segmentation is done by selecting fixed length windows of 130 and 600 ms, respectively. The QRS complex time window is centered around the fiducial point. The ST-T complex time window starts from a heart rate related sample reference. Short ST-T waveforms are extended up to 600 ms by appending zeros.

2) KLT coefficient series: The beat-to-beat dynamic evolution of the signal is characterized by the study of the coefficient time series evolution. We have used a set of KLT basis for the QRS complex and the ST-T waveform derived from more than 200000 preprocessed and selected waveforms as described in [5].

The four most important coefficient series for each interval were derived by projecting each segmented QRS/ST-T complex over the the first four KLT QRS/ST-T basis. They are referred to as α_k^l, where l denotes lead and k KLT order.

Distance functions, denoted φ_l^{QRS} and φ_l^{STT}, are derived for each lead l. These functions are basically the distance series between each KLT coefficient series and a mean reference value ($\alpha_k^l[r]$) estimated using the first 20 samples of the series.

$$\varphi_l[n] = \left(\sum_{k=1}^{4} \left(\alpha_k^l[n] - \alpha_k^l[r] \right)^2 \right)^{1/2}, \quad l \in \{X, Y, Z\} \qquad (1)$$

where $\alpha_k^l[n]$ is the k-th order coefficient of beat n estimated from the lth lead.

3) GLRT-based Detector Stage: Step-like changes in the KLT coefficient series have been observed when postural changes occur. This observation is translated to a detection problem where a step-like pattern is searched for in the observation window, and then a sliding window approach will be used in the whole recording.

The distance function $\varphi_l[n]$, computed for lead l, is considered for determining whether a BPC has occurred (hypothesis $\mathcal{H}_1$) or only noise is present (hypothesis $\mathcal{H}_0$). The onset of the observation interval occurs at the sliding time instant $n = n_0$. A BPC is characterized by the scaled unitary step-like signature $s[n]$ which is disturbed by an additive, Laplacian signal (noise) $w_l[n]$ with mean value m_l. This m_l can be interpreted as the DC level of $\varphi_l[n]$ within the observation window. The signal model is summarized as follows:

$$\begin{aligned} \mathcal{H}_0 :\ \varphi_l[n] &= w_l[n] && n = n_0, ..., n_0 + D - 1 \\ \mathcal{H}_1 :\ \varphi_l[n] &= a_l \cdot s[n - n_0] + w_l[n] && n = n_0, ..., n_0 + D - 1 \end{aligned} \quad (2)$$

where $l = 1, ..., L$ represents the lead where $\varphi_l[n]$ is computed, a_l is the scaling factor of the unitary step-like function $s[n]$ and D represents the length of the observation window. $\boldsymbol{\varphi} = [\boldsymbol{\varphi}_1\ \boldsymbol{\varphi}_2\ ...\ \boldsymbol{\varphi}_L]^T$ is a $L \times D$ matrix and represents information related to each of the orthogonal leads.

The signal $s[n]$ is modeled as a step-like change:

$$s[n] = \begin{cases} 1 & \text{if } n = 0, ..., \frac{D}{2} - 1 \\ -1 & \text{if } n = \frac{D}{2}, ..., D - 1 \end{cases} \quad (3)$$

where the length of $s[n]$ is an even-valued integer D. A BPC is manifested in $\varphi_l[n]$ by either a positive or negative shift, with equal probability. Therefore, the scaling factor of the transition, a_l, is positive for a negative shift and negative for for a negative one. The absolute value of a_l represents half of the shift due to the BPC.

The additive noise w_l is supposed to be Laplacian with mean m_l and variance σ^2. All variables are assumed to be mutually independent and uncorrelated to the observation signal $\varphi_l[n]$.

By using the Laplacian distribution, the generalized likelihood ratio test (GLRT) rejects $\mathcal{H}_0$ if:

$$\Lambda_G(\boldsymbol{\varphi}) = \frac{p(\boldsymbol{\varphi}; \widehat{a}_{l,\mathcal{H}_1}, \widehat{m}_{l,\mathcal{H}_1}, \mathcal{H}_1)}{p(\boldsymbol{\varphi}; \widehat{m}_{l,\mathcal{H}_0}, \mathcal{H}_0)} =$$

$$\frac{\exp\left[-\sqrt{\frac{2}{\sigma^2}}\sum_{l=1}^{L}\sum_{n=n_0}^{n_0+D-1}\left|\varphi_l[n] - \widehat{m}_{l,\mathcal{H}_1} - \widehat{a}_{l,\mathcal{H}_1} s[n-n_0]\right|\right]}{\exp\left[-\sqrt{\frac{2}{\sigma^2}}\sum_{l=1}^{L}\sum_{n=n_0}^{n_0+D-1}\left|\varphi_l[n] - \widehat{m}_{l,\mathcal{H}_0}\right|\right]} > \gamma \quad (4)$$

where $\widehat{a}_{l,\mathcal{H}_i}$ and $\widehat{m}_{l,\mathcal{H}_i}$ denote their MLE under the hypothesis $\mathcal{H}_i$. The unknown $\widehat{m}_{l,\mathcal{H}_i}$ is regarded as nuisance parameter.

Calculation of the MLE of $m_{l,\mathcal{H}_0}$:

$$\widehat{m}_{l,\mathcal{H}_0} = \text{med}(\varphi_l[n_0], ..., \varphi_l[n_0 + D - 1]) \quad (5)$$

Calculation of the MLE of $m_{l,\mathcal{H}_1}$ and $a_{l,\mathcal{H}_1}$:

The MLE of $m_{l,\mathcal{H}_1}$ and $a_{l,\mathcal{H}_1}$ under $\mathcal{H}_1$ are obtained by minimizing the cost function $J(m_{l,\mathcal{H}_1}, a_{l,\mathcal{H}_1})$:

$$J(m_{l,\mathcal{H}_1}, a_{l,\mathcal{H}_1}) = \sum_{n=n_0}^{n_0+D-1} |\varphi_l[n] - m_{l,\mathcal{H}_1} - a_{l,\mathcal{H}_1} \cdot s[n - n_0]| \quad (6)$$

To do so, both $\frac{\partial J}{\partial m_{l,\mathcal{H}_1}}$ and $\frac{\partial J}{\partial a_{l,\mathcal{H}_1}}$ should be set to zero:
For $m_{l,\mathcal{H}_1}$:

$$\frac{\partial J}{\partial m_{l,\mathcal{H}_1}} = -\sum_{n=n_0}^{n_0+D-1} sgn(\varphi_l[n] - m_{l,\mathcal{H}_1} - a_{l,\mathcal{H}_1} \cdot s[n - n_0]) \quad (7)$$

and this is set to zero when:

$$\widehat{m}_{l,\mathcal{H}_1} = \text{med}(\varphi_l[n] - a_{l,\mathcal{H}_1} \cdot s[n - n_0]) \quad \text{for } n = n_0, ..., n_0 + D - 1 \quad (8)$$

The signal $(\varphi_l[n] - a_{l,\mathcal{H}_1} \cdot s[n - n_0])$ represents, under $\mathcal{H}_1$, the Laplacian random signal $w_l[n]$, which is centered at m_l (see PDF in Fig. 1(a) and eq. (2)).

The PDF of $\varphi_l[n]$ can be interpreted under $\mathcal{H}_1$ as two sub-PDFs: the w_l one shifted $+a_l$ and the same shifted $-a_l$. Then, we can see the PDF of $\varphi_l[n] - a_{l,\mathcal{H}_1}\ s[n - n_0]$ as the PDF of the signal $\varphi_l[n]$ shifted $+a_{l,\mathcal{H}_1}$ and $-a_{l,\mathcal{H}_1}$, see Fig. 1. Therefore, the median value of $\varphi_l[n] - a_{l,\mathcal{H}_1}\ s[n - n_0]$ could be replaced by the median value of $\varphi_l[n]$, which would not require any knowledge of a_l. This replacement to estimate m_l from Fig. 1(b) suffers from the fact that the PDF of the signal $\varphi_l[n]$ has few data which cause a big uncertainty. Therefore, $\widehat{m}_{l,\mathcal{H}_1} = \text{med}(\varphi_l[n])$ will be used as an initial estimate, and will then be iterated (see below).

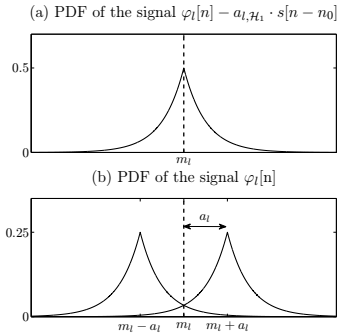

Fig. 1. (a) PDF of $\varphi_l[n] - a_{l,\mathcal{H}_1} \cdot s[n - n_0]$. (b) PDF of the signal $\varphi_l[n]$.

For $a_{l,\mathcal{H}_1}$:

$$\begin{aligned} \frac{\partial J}{\partial a_{l,\mathcal{H}_1}} &= -\sum_{n=n_0}^{n_0+D-1} s[n - n_0] sgn(\varphi_l[n] - m_{l,\mathcal{H}_1} - a_{l,\mathcal{H}_1} s[n - n_0]) = \\ &\underset{using(3)}{=} -\sum_{n=n_0}^{n_0+D/2-1} sgn(\varphi_l[n] - m_{l,\mathcal{H}_1} - a_{l,\mathcal{H}_1}) - \\ &\quad \sum_{n=n_0+D/2}^{n_0+D-1} -1 \cdot sgn(\varphi_l[n] - m_{l,\mathcal{H}_1} + a_{l,\mathcal{H}_1}) \end{aligned} \quad (9)$$

If we replace $\widetilde{\varphi}_l[n - n_0] = \varphi_l[n] - m_{l,\mathcal{H}_1}$:

$$\begin{aligned} \frac{\partial J}{\partial a_{l,\mathcal{H}_1}} &= \\ &= -\sum_{n=n_0}^{n_0+D/2-1} sgn(\widetilde{\varphi}_l[n] - a_{l,\mathcal{H}_1}) - \sum_{n=n_0+D/2}^{n_0+D-1} -sgn(\widetilde{\varphi}_l[n] + a_{l,\mathcal{H}_1}) \\ &= -\sum_{n=n_0}^{n_0+D/2-1} sgn(\widetilde{\varphi}_l[n] - a_{l,\mathcal{H}_1}) - \sum_{n=n_0+D/2}^{n_0+D-1} sgn(-\widetilde{\varphi}_l[n] - a_{l,\mathcal{H}_1}) \\ &= -\sum_{n=n_0}^{n_0+D-1} sgn(\widetilde{\varphi}_l[n] \cdot s[n - n_0] - a_{l,\mathcal{H}_1}) \end{aligned} \quad (10)$$

Thus, the MLE of $a_{l,\mathcal{H}_1}$ is:

$$\widehat{a}_{l,\mathcal{H}_1}=\text{med}((\varphi_l[n]-m_{l,\mathcal{H}_1})s[n-n_0]) \quad n=n_0,..,n_0+D-1 \quad (11)$$

Note that both $\widehat{m}_{l,\mathcal{H}_1}$ and $\widehat{a}_{l,\mathcal{H}_1}$ have to be estimated jointly, using alternating optimization. A proper initial estimate for $m_{l,\mathcal{H}_1}$ has been shown in Fig. 1 to be the median of $\varphi_l[n]$. This is then included in (11) to estimate $\widehat{a}_{l,\mathcal{H}_1}$, which is included (8) and so on until convergence. They all converge, most of them in less than 10 iterations.

4) GLRT detector $\mathrm{T}(\boldsymbol{\varphi_l})$*:* Once $\widehat{m}_{l,\mathcal{H}_0}$, $\widehat{m}_{l,\mathcal{H}_1}$ and $\widehat{a}_{l,\mathcal{H}_1}$ have been obtained, logarithms of both sides in the equation (4) are taken, resulting in:

$$\ln \Lambda_G(\varphi_l) = -\sqrt{\frac{2}{\sigma^2}}\sum_{n=n_0}^{n_0+D-1}\left(|\varphi_l[n]-\widehat{m}_{l,\mathcal{H}_1}-\widehat{a}_{l,\mathcal{H}_1}s[n-n_0]|-|\varphi_l[n]-\widehat{m}_{l,\mathcal{H}_0}|\right) \quad (12)$$

Thus, the detector becomes:

$$\mathrm{T}(\boldsymbol{\varphi_l})=\sum_{n=n_0}^{n_0+D-1}\left(|\varphi_l[n]-\widehat{m}_{l,\mathcal{H}_0}|-|\varphi_l[n]-\widehat{m}_{l,\mathcal{H}_1}-\widehat{a}_{l,\mathcal{H}_1}s[n-n_0]|\right)$$

$$\mathrm{T}(\boldsymbol{\varphi_l}) \underset{\mathcal{H}_0}{\overset{\mathcal{H}_1}{\gtrless}} \sqrt{\frac{\sigma^2}{2}}\ln(\gamma) \quad (13)$$

As σ is assumed to be constant, $\sqrt{\frac{\sigma^2}{2}}\ln\gamma$ is comprised in a new threshold γ'.

The GLRT-based detector is applied to each of the six distance functions $\varphi_l^{\text{QRS}}[n]$ and $\varphi_l^{\text{STT}}[n]$, where l=[X, Y, Z], normalized by the square root of the mean energy of the complex in each lead, obtained from the first 50 beats of the recording. The obtained detection outputs (see Fig. 2), $\mathrm{T}(\varphi_l^{\text{QRS}}[n])$ and $\mathrm{T}(\varphi_l^{\text{STT}}[n])$ are combined as described in the following equation:

$$\mathrm{T}[n]=\sum_{l=1}^{3}(\lambda_{\text{QRS}}\cdot\mathrm{T}(\varphi_l^{\text{QRS}}[n])+\lambda_{\text{STT}}\cdot\mathrm{T}(\varphi_l^{\text{STT}}[n])) \quad (14)$$

where λ_{QRS} and λ_{STT} represent the weights of the QRS and STT detection outputs.

Although the largest changes during BPCs are usually related to the QRS complex it is also desirable to also account for changes in the ST-T waveform. Therefore, the weights $\lambda_{\text{QRS}}=0.8$ and $\lambda_{\text{STT}}=0.2$ were selected [3].

In order to handle the detection of several BPCs, the detector $\mathrm{T}(\boldsymbol{\varphi})$ repeats the GLRT in successive, overlapping intervals of length D, i.e a sliding window, until the entire signal has been processed. The corresponding length of $s[n]$, D, is set to 44 samples which correspond to 44 s since all the distance functions are sampled to 1 Hz.

5) Decision Stage: We apply a fixed threshold set to 0.55, to the combined output $T[n]$, and thus, both the beginning and the end of a single BPC may be detected as two separate events. In case there are more than one peak detected, we choose the first one in the interval which is the maximum within a window of 40.

Stable intervals in the KLT coefficient series before and after a BPC are also produced, causing flat intervals in the detector output. Then, BPCs with widths that exceed 55 s and widths at one quarter of the maximum height between 19 and 39 are excluded to force such stable intervals.

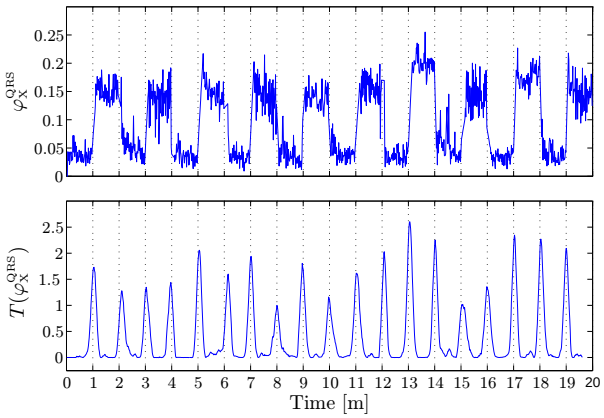

Fig. 2. Example of the output of the detector.

A refractory period which excludes detections within a time interval of 10 s following the most recent detection is included in the decision algorithm.

6) Noise Stage: An extra stage is considered after analysing the results, to be added to the detection scheme. The idea consists of making use of the information contained in the noisy beats which are rejected from the study and the SNR estimated in the preprocessing stage, due to the fact that all recordings of the BPC database present a very low SNR during a BPC as exemplified in Fig. 3.

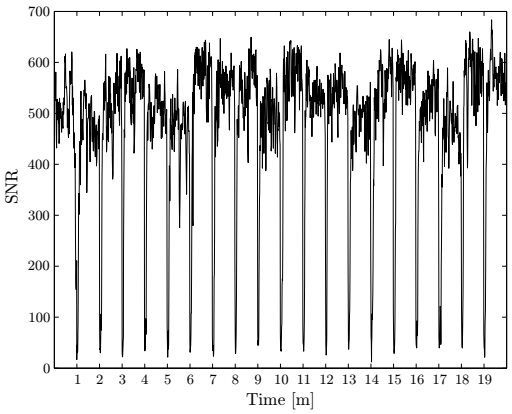

Fig. 3. Example of the SNRs calculated in the φ_X^{QRS}.

B. Reference Material

The evaluation of the GLRT-based BPC detector is performed in two databases with respect to the following aspects: first, the ability of the system to detect BPCs, and second, the false alarm rate of BPCs in ischemic episodes. In both databases the standard 12-lead ECG was recorded with a sampling rate of 1 kHz and an amplitude resolution of 0.6 μV. Both were used for training and testing.

1) Healthy subjects: BPC database: The performance of the BPC detector is studied on an ECG database consisting of 20 subjects (11 males/9 females, 32±9 years old). The

BPC database was recorded following the protocol: supine-to-right side, supine-to-left side and so on. The complete sequence was repeated five times with a duration of 1 min per BPC in order to give more reliable statistical results [3], [6].

2) Subjects undergoing PCI: STAFF III database: The second database contains severe induced ischemic events [7]. The study group consisted of 83 patients undergoing a percutaneous coronary intervention (PCI), where a balloon is inflated, blocking the artery in one of the major coronary arteries. A control ECG recorded prior to the procedure, and the angioplasty ECG were considered for each patient, and denoted with (c) and (a), respectively. It is assumed that no BPCs occurred during the recording of this data.

III. RESULTS

The performance of the proposed detector is assessed in terms of sensitivity (S) and positive predictivity value ($+PV$) with average statistics (av), that assigns the same weight to each recording, for the BPC database. For the STAFF-III database, where it is assumed that there are no BPCs, performance is assessed in terms of the false alarm rate defined as the number of false BPCs per hour. Performance of the GLRT-based detector assuming Laplacian noise is compared to the performance of a reimplementation of the GLRT detector assuming Gaussian noise [3], [6]. Also, the performance obtained in [3], [6], which used different ad hoc rules is shown in Table I. In those studies, the median absolute deviation (MAD) [8] was used for outlier rejection. Results of these three strategies (Laplacian, Gaussian and Gaussian with MAD) and the original implementation of Gaussian with MAD in [3], [6], with and without the noise rejection stage, are presented in Table I.

	BPC database		STAFF III database	
	S(av)	*+PV(av)*	$R_{FA}(c)$	$R_{FA}(a)$
WITHOUT NOISE STAGE				
Laplacian	94.2%	97.3%	13.2 ± 16.0	14.1 ± 9.2
Gaussian	83.4%	95.2%	14.2± 14.1	11.9 ± 11.1
Gaussian (with MAD)	88.9%	96.7%	13.9± 14.3	12.1 ± 10.0
Gauss (MAD) [6], [3]	89%	97%	4 ± 13	11 ± 14
WITH NOISE STAGE				
Laplacian	92.6%	99.3%	2.5 ± 7.2	1.7 ± 4.0
Gaussian	82.1%	99.7%	1.9 ± 5.8	1.4 ± 4.0
Gaussian (with MAD)	85.3%	99.4%	2.2 ± 5.7	0.9 ± 2.8
Gauss (MAD) [6], [3]	90%	99%	1 ± 3	2 ± 7

TABLE I

PERFORMANCE STATISTICS FOR THE BPC DETECTORS ON THE BPC AND STAFF III DATABASES. THE FALSE ALARM RATES $R_{FA}(a)$, AND $R_{FA}(c)$ ARE EXPRESSED IN TERMS OF MEAN AND STANDARD DEVIATION.

The Laplacian-based detector performs very well on the BPC database ($S/+PV$: 94.2%/97.3%). However, when the detector is applied to the STAFF III database where no BPCs are supposed to occur, the performance is reduced to about $R_{FA}(a)$=14 false alarms per hour. Some angioplasty recordings contain sudden step changes in the KLT coefficient series, needing the noise stage in order to remove the false BPC detections.

The performance assuming Gaussian noise and using the GLRT detector published in [3], [6] decreases.

As expected, when including the noise stage after the detection algorithm, S decreases to 92.6% and $+PV$ increase in the BPC database to 99.3%. In the case of the STAFF III database, the number of false BPCs decrease considerable to $R_{FA}(c)$=2.5 and $R_{FA}(a)$=1.7 episodes per hour.

IV. DISCUSSION

Performance of the GLRT-based detector for Laplacian noise has improved from 85% to 92.6% in sensitivity for the same specificity, with respect to a detector which assumed Gaussian distribution with the MAD filter presented in [6]. Results in the original implementation [6], [3] are higher because some different ad hoc rules which were used. Now, those have been simplified with the Laplacian detector. However, when comparing to the original implementation, we still obtain a 2% increase in sensitivity.

In the case of angioplasty recordings, where there is a complete cessation of blood flow through a coronary artery, sudden changes in the ECG are produced, and those result in step like changes in the KLT of the QRS and STT complexes. However, those events are not likely to come from BPCs.

The false alarm rate significantly decreased when the noise stage was included in the detection (from 14 to 2 detections per hour). However, although the false alarm rate in the control recordings (same subjects who underwent the percutaneous coronary intervention) is higher than during the PCI recordings. This could be explained because during the control recording, subjects were awaken and some postural changes could have taken place.

In the angioplasty recordings, the occlusion is complete and very fast, while most of the ischemic events have a softer transient signature in the KLT coefficient series of the QRS and STT complexes. Then, the false alarm rate would be lower in ambulatory recordings or in ST monitoring, which are the targets, where ischemic events are less severe.

REFERENCES

[1] M. G. Adams and B. J. Drew, "Body position effects on the ECG: Implication for ischemia monitoring," *J Electrocardiol*, vol. 30, no. 4, pp. 285–291, 1997.

[2] B. L. Nørgaard, B. M. Rasmussen, M. Dellborg, and K. Thygesen, "Positional changes of spatial QRS- and ST-segment variables in normal subjects: implications for continuous vectorcardiography monitoring during myocardial ischemia," *J Electrocardiol.*, vol. 33, no. 1, pp. 23–30, 2000.

[3] J. García, M. Åström, J. Mendive, P. Laguna, and L. Sörnmo, "ECG-based detection of body position changes in ischemia monitoring," *IEEE Trans Biomed Eng*, vol. 25, no. 6, pp. 501–507, 2003.

[4] G. Moody and R. Mark, "Development and evaluation of a 2-lead ECG analysis program," in *Computers in Cardiology*, (Los Alamitos), pp. 39–44, IEEE Comput. Soc. Press, 1982.

[5] J. García, P. Lander, L. Sörnmo, S. Olmos, G. Wagner, and P. Laguna, "Comparative study of local and Karhunen-Loève-based ST-T indexes in recordings from human subjects with induced myocardial ischemia," *Comput. Biomed. Res.*, vol. 31, no. 4, pp. 271–292, 1998.

[6] M. Åström, J. García, P. Laguna, O. Pahlm, and L. Sörnmo, "Detection of body position changes using the surface electrocardiogram," *Med Biol Eng Comput*, vol. 41, no. 2, pp. 164–171, 2003.

[7] J. García, P. Lander, L. Sörnmo, S. Olmos, G. Wagner, and P. Laguna, "Comparative study of local and Karhunen-Loeve based ST-T indexes in recordings from human subjects with induced myocardial ischemia," *Comput. Biomed. Res.*, vol. 31, pp. 271–292, 1998.

[8] F. Hampel, E. Ronchetti, P. Rousseeuw, and W. Stahel, *Robust Statistics*. Probability and Mathematical Statistics, New York: Wiley,, 1986.